NASA Technical Memorandum 106459
AIAA–94–0799

Characteristics of Surface Roughness Associated With Leading Edge Ice Accretion

Jaiwon Shin
Lewis Research Center
Cleveland, Ohio

Prepared for the
AIAA 32nd Aerospace Sciences Meeting and Exhibit
sponsored by the American Institute of Aeronautics and Astronautics
Reno, Nevada, January 10–13, 1994

CHARACTERISTICS OF SURFACE ROUGHNESS ASSOCIATED WITH LEADING EDGE ICE ACCRETION

Jaiwon Shin*
National Aeronautics and Space Administration
Lewis Research Center
Cleveland, Ohio 44135

Abstract

Detailed size measurements of surface roughness associated with leading edge ice accretions are presented to provide information on characteristics of roughness and trends of roughness development with various icing parameters. Data was obtained from icing tests conducted in the Icing Research Tunnel (IRT) at NASA Lewis Research Center (LeRC) using a NACA 0012 airfoil. Measurements include diameters, heights, and spacing of roughness elements along with chordwise icing limits. Results confirm the existence of smooth and rough ice zones and that the boundary between the two zones (surface roughness transition region) moves upstream towards stagnation region with time. The height of roughness grows as the air temperature and the liquid water content increase, however the airspeed has little effect on the roughness height. Results also show that the roughness in the surface roughness transition region grows during a very early stage of accretion but reaches a critical height and then remains fairly constant. Results also indicate that a uniformly distributed roughness model is only valid at a very initial stage of the ice accretion process.

Nomenclature

k	measured roughness height, mm
k_c	critical roughness height inducing a boundary layer transition, mm
k_s	sand grain roughness height, mm
s	distance along the surface, mm
t	accretion time, minute
V_∞	airspeed, m/s

Introduction

It is a well known fact that iced surfaces develop roughness during an ice accretion process. Surface roughness elements modify the local collection efficiency over the elements themselves and affect local convective heat transfer rates, which in turn affects the overall ice shape. Surface roughness also has an important effect on development of the boundary layer. Despite the importance, there has not been much work done to investigate the surface roughness associated with ice accretion.

With a lack of empirical correlations that can be used to evaluate the effect of roughness elements found on typical ice accretions, it has become standard practice in current ice accretion prediction methods to develop an empirical correlation for either the surface element roughness height or the convective heat transfer coefficient. These correlations are developed by first predicting the ice shapes for a set of experimental ice shapes by changing the roughness element height (or the convective heat transfer coefficient) to determine the value that yields the best agreement with experiment.

This type of approach raises several concerns. First, empirical correlations developed by this approach do not reflect ice accretion physics or actual surface conditions, and they are dependent on the numerical algorithm. Secondly, these empirical correlations relate the sand grain roughness height to the icing parameter, using the concept of equivalent sand grain roughness stemming from work of Nikuradse (Ref. 1) and Schlichting (Ref. 2). Although, this type of roughness has been widely used for many applications in fluid mechanics and a large amount of experimental data is available, surface roughness characteristics associated with ice accretions are very different from conventional roughness types such as the sand grain roughness in both size and distribution. These concerns precipitated a need for development of a better physical roughness model for ice accretion prediction methods.

For the development of a better physical roughness model, there have been several studies (Refs. 3 to 6) to increase an understanding of the surface roughness physics. However, previous studies have dominantly been observational and qualitative through a use of close-up photography or videography. The most detailed work on the leading edge surface roughness has been documented by Hansman, et al. (Ref. 4) on a cylinder. Results showed that there are a smooth and a rough zone on the surface and the rough zone propagates towards the stagnation region with time. Hansman speculated that surface tension effects caused coalescence of surface

*Aerospace Engineer, Member AIAA

water into stationary beads. And these beads in the boundary region between the smooth and the rough zone caused a boundary layer transition, which enhances heat transfer in the region so that water beads freeze faster. This sudden change in the surface condition from a smooth surface with no noticeable roughness to a rough surface indicates that there must be underlying physics. Understanding this physics is critical for the study of roughness formation and its interaction with the boundary layer. In order to understand the roughness effects on the boundary layer in this region, detailed boundary layer measurements are necessary over the iced surface with realistic roughness. However, there has not been any work providing quantitative data describing size and distribution of roughness for boundary layer measurement tests to use. The objective of the current study is to fill this gap and bring more insights for roughness model development efforts.

As an initial effort, it is important to investigate effects of icing parameters on development of roughness, because understanding such effects could shed a light on the correct approach to a model development effort. The results can also be very valuable in assessing needs for modification of current roughness models, and for estimating roughness heights and surface conditions. This information is also useful for designing simulated ice shapes for various wind tunnel and flight tests studying aerodynamic degradation due to ice accretion. Development of a boundary layer is affected by the presence of surface roughness, and this adds to changes in lift and drag characteristics of an airfoil due to the ice accretion. Therefore, it is desired that the surface condition be replicated as close to the actual ice accretion as possible for these simulated tests. There have been several investigations (Refs. 7 to 9) to study icing effects on airfoil lift and drag. The majority of the work used a uniform size of grain roughness over the surface, which is quite different from the roughness characteristics in real ice accretions.

In the following, experimental investigations focused on the quantification of surface roughness for glaze ice will be presented as well as a test technique and a data analysis method developed for the current study.

Test Method

Icing Research Tunnel

The NASA LeRC IRT is a closed-loop refrigerated wind tunnel. A 5000 hp fan provides airspeeds up to 134 m/sec (300 mph). The refrigeration heat exchanger can control the total temperature from −1.1 to −42 °C. The spray nozzles provide droplet sizes from approximately 10 to 40 μm median volume droplet diameters (MVD) with liquid water contents (LWC) ranging from 0.2 to 3.0 g/m^3. The test section of the tunnel is 1.83 m (6 ft) high and 2.74 m (9 ft) wide.

Test Model

To eliminate any geometry related effects on development of roughness characteristics, a generic airfoil with a moderate leading edge radius was chosen. The airfoil had a 0.53 m (21 in) chord and a 1.83 m (6 ft) span with a cross section of a NACA 0012 airfoil. The airfoil was made of aluminum and the surface was finished to be aerodynamically smooth. The model was mounted vertically in the center of the test section and set at a 0° angle-of-attack for the entire test.

Test Condition

Test conditions were selected to study the effects of airspeed, air temperature, LWC, and accretion time on the surface roughness. Test conditions are listed in Table 1. The conditions are focused mainly to produce glaze ice since roughness and heat transfer are much more important in the glaze ice regime. For this reason, tests were conducted mostly near the freezing point, namely −1.1, −2.2, and −3.9 °C in total temperature.

Several ice accretion times were tested to study the development of roughness with time. Accretion times were typically 2 and 6 min, and several other accretion times were tested for selected conditions.

Data Acquisition Method

There were three requirements for the data acquisition method to meet the objective of the test. First, the method should be able to provide detailed and accurate enough data for measurements of the roughness element size which is on the order of a millimeter. Second, the method should be able to provide fast acquisition and processing capabilities to handle a large size database for studying the trend of roughness characteristics with icing parameters. Third, the method should not alter the surface condition during a data acquisition process. With these concerns, an optical imaging technique was chosen over other mechanical measurement techniques. Each iced surface was photographed using a KODAK digital camera system with a 60 mm macro lens to capture detailed surface roughness characteristics. Images were later transmitted to a personal computer for measurements. Actual measurements of roughness elements were done using an image processing program.

In addition to digital images, ice shapes and section drag were documented. Ice shapes were traced on cardboard templates at the mid-span using a pencil. The section drag at the mid-span of the airfoil was calculated from total pressure profiles measured by a pitot-static wake survey probe. Ice shapes and section drag coefficient results can be useful for validation work for ice accretion codes and performance codes. For the scope of this paper, the results on the ice shape tracing and section drag are not included here.

Test Procedure

Since the use of the digital camera requires a close access to the iced surface, it was necessary to bring the tunnel to idle for test personnel to go into the test section for data acquisition after a desired spray.

A typical test procedure for icing runs is listed below.

1. The target airspeed and total temperature were set.
2. The spray system was adjusted to the desired MVD and LWC.
3. The spray system was turned on for the desired spray time.
4. The wake survey was traversed across the airfoil wake with the tunnel at the target airspeed.
5. The tunnel was brought down to idle again for digital photo data and ice shape tracings.
6. The airfoil was then cleaned and the tunnel conditions set for the next data point.

Image Data Acquisition and Analysis

Digital Camera System

A KODAK Digital Camera System (DCS) was used to document detailed surface conditions. The camera system consisted of a camera and a digital image storage unit. The camera uses a conventional 35 mm film camera body with a solid sensor replacing a film pack. The camera is equipped with a RS-232 serial port to send images to the storage unit. The storage unit is essentially a small computer with a hard drive for image storage. It also has a RS-232 serial port for transmitting images to a computer. The resolution of the camera is 1024 x 1280 pixels. The system is capable of taking color images and the operation is much like that of a conventional 35 mm film camera. The KODAK Co. provides an interface program that allows images to be read by an image processing program (Ref. 10) running on Macintosh personal computers.

Image Processing

Two types of digital images were taken in order to capture both base and height dimensions of roughness elements. For diameter and spacing measurements, the lens was aimed normal to the surface to obtain a plan view (Fig. 1). For height measurements, the lens was aimed parallel to the surface to reveal the profile of roughness elements (Fig. 2).

Once an image is transmitted to a computer, the image is enhanced by using the image processing program (Ref. 10) for better contrast and sharpness. This enhancement does not alter the data. The enhanced image is then read in by another software (Ref. 11) which is capable of making many measurements of objects in the image including the length and angle. The software requires a reference scale in the image to calibrate pixels to a physical length. The reference scale is provided by a ruler placed over the ice as shown in Figs. 1 and 2. After the pixels are calibrated for a known length, sizes of roughness elements are measured and the data is stored in a tabular format with identification numbers relating measured values to corresponding elements in the image. These identification numbers can be stamped in the image for future reference.

Accuracy of the System

When an imaging technique is used to obtain quantitative information, the technique needs to be validated for any possible errors caused by optical instruments or image processing. In order to document the accuracy of the data acquisition and image analysis technique, several images of the clean airfoil surface were taken using the same lens, camera setting, and lighting as during the test. The image included two rulers used during the test and a cross with each line being 10 mm long in between the rulers. Since all images were taken in a static environment during the test, no dynamic validation is needed.

There are largely two sources where possible errors could occur; errors involved with the data acquisition and measurement systems and errors caused by a human during data reduction processes.

System Error

System errors for the current work can come form the optical distortions, inaccuracy of the rulers, and the fact that the airfoil surface is not flat. In order to minimize any optical distortions, the following precautions were taken. Images were always taken with the lens aiming normal to the surface for plan view images (Profile images do not have this concern.), and the area of interest was always placed in the center of the field of view.

For most of the images used for data, the focused area occupied only about the center 30 percent of the whole image. This was purposely done by using a lens with a very small depth of field. Since only the focused area was used for actual measurements by cropping it from the whole image, a concern about optical distortion in the image corners is eliminated.

Typically a focused image was 5 mm wide along the surface and 15 mm long in the spanwise direction. A concern is then how much warping occurs within the focused field of view in both chordwise and spanwise directions. The warping in the chordwise direction is a bigger concern for plan view images because of the curvature of the airfoil surface. For the height measurement, spanwise distortion is the only concern because the small depth of field helped to separate elements which are not in the same plane with the reference ruler by making those elements out of focus. Chordwise distortion was documented by calculating the surface curvature over a 6 mm wide surface. This surface location corresponds to a typical surface roughness transition region where most of the measurements were made. Results showed that an error introduced by the curvature was calculated to be 0.005 mm for a 1 mm length. Because of the curved airfoil surface, it is important to use a portion of

the ruler in the center of the image as a reference scale for calibration. Spanwise distortion was documented by making several measurements of 1 mm scales of two rulers in the validation image, since the rulers were placed about 20 mm apart from each other in the spanwise direction. Results showed no difference in measured values indicating that there is no sizable spanwise distortion with an image size used in this study.

The accuracy of the rulers used during the test was not pursued any further than measuring the scales with a vernier calipers. For calibrating pixels, a millimeter scale in the center of the image was used during the measurement process. Millimeter scales were accurate within ±0.05 mm.

Human Error

Although the image acquisition and analysis systems are proven to be accurate, there could be an error involved with a user. The image processing program requires a user to click two points in the image to calculate a linear distance between them. A few pixels can be added to or subtracted from the total number of pixels in the distance depending on where the two end points are defined. An exercise was performed to test a user's ability for consistency. The repeatability check showed the error is bounded within 2 pixels. More than 70 percent of the repeatability measurements showed no error and a two-pixel error occurred in less than 10 percent. One pixel translates roughly to 0.03 mm with the magnification used, however the magnification varies somewhat in each image.

Based on the error analyses, it is found that the system error is negligible compared with a possible user error. Therefore, the maximum possible total error in a measurement is estimated to be about two pixels, which translates roughly to 0.06 mm.

Results and Discussions

A majority of measurements for the roughness size were made in the region where the rough zone begins aft of the smooth zone. This region will be referred to as the surface roughness transition region because it is the region where surface condition changes from a smooth one to a rough one. The results from this region are used to study icing parameter effects and accretion time effects on the roughness size as will be discussed in the following. Reasons for selecting this surface location for the measurements will be discussed later after the results are presented.

Effects of Icing Parameters

The results in this section present roughness size measurements for various airspeeds, air temperatures, and LWCs to illustrate the effects of these icing parameters on the roughness size. All the ice accretions used for the data are for 2 min accretions. During the tests, there were conditions to investigate the effect of MVD on the roughness, however many of the digital images for this portion of the test turned out to be out of focus so that a complete data set for analysis was not available. For this reason, the effect of the MVD is not presented in this paper.

Measurements were made for the height, diameter and spacing of roughness elements for three airspeeds (67.1, 89.5, and 111.8 m/s), three air temperatures (−1.1, −2.2, and −3.9 °C in total temperature), and four LWCs (0.5, 0.75, 1.0, and 1.2 g/m^3). With each dimension, a number of measurements were made and a statistical analysis was made to obtain a mean value. Mean values of the diameter, height, and spacing are listed in Table 2 for all the ice accretions used for the measurement. The number of samples vary among the ice accretions, so standard deviations are listed in a parenthesis to give an idea about the spread of the measured values. Also included is the width of smooth zone which is measured from the stagnation line to the beginning of the rough zone. Roughness elements are hemispheres unless otherwise noted.

The results are compared with the prediction by the current roughness model used in the LEWICE code (Ref. 12). LEWICE uses an empirical correlation developed for the roughness element height. The experimental data used to develop this correlation was obtained by Gent (Ref. 13), which had a geometrically similar airfoil, the same LWC and MVD values as the current study. This data set showed the effect of velocity, LWC, and static temperature on the shape of the ice accretion formed. The effects of droplet diameter, body geometry, static pressure, etc. have not been included in the correlation.

Figure 3 shows measured roughness heights from the current study and predicted sand grain roughness heights from the LEWICE model plotted against the airfoil surface distance. Note that absolute values of roughness heights are not to be meant for direct comparison since one is an actual roughness height and the other is an equivalent sand grain roughness height. Trends are the same between the measured height and the predicted height except for the airspeed. The current results show almost constant roughness height with increasing airspeed whereas the LEWICE roughness model predicts growth of the roughness height with airspeed. This insensitivity of roughness height with airspeed was found during numerical studies by Shin, et al. (Ref. 14) earlier. In that study, it was shown that a change of roughness height due to a change in the airspeed resulted a minimal change on the ice shape. Although the roughness height remains almost constant, its height relative to the boundary layer thickness grows with the airspeed since the boundary layer becomes thinner as the airspeed increases. This will be more evident in a following discussion (Figs. 4(a) to (c)). One other noteworthy observation is that for the effect of LWC, the growth rate of the roughness height predicted by the LEWICE model is much higher than the one suggested by the current result.

Figure 4 shows comparisons of the measured roughness height with the predicted laminar boundary layer thickness and with the predicted critical roughness height to cause a transition. Bragg, et al. calculated the boundary layer thickness and critical roughness heights for this present paper, and their method is described in detail in Ref. 15. The boundary layer thickness results are for a clean NACA 0012 airfoil and the critical roughness height was calculated based on an assumption that the boundary layer transition occurs due to a presence of a single hemisphere at each plotted location. So, the figure indicates that if the roughness height is bigger than the critical roughness height at a given surface location, a transition is likely to occur. Also plotted are the measured roughness heights at surface locations where these measurements were made, namely the beginning of the rough zone.

As mentioned, the boundary layer thicknesses in Fig. 4 are for a clean airfoil, so they do not account for geometry changes at the leading edge made by 2 min ice accretions or effects caused by surface roughness. However, for small ice accretions with no horns such as the ones used here, a geometry change due to an ice accretion near the stagnation region would be very close to outward displacement of the airfoil leading edge. Also, the boundary layer would develop over a fairly smooth iced surface until it reaches the surface roughness transition region where roughness starts to form and where the measurements were made. Therefore, a clean airfoil boundary layer thickness may be used as an acceptable estimate for a boundary layer thickness over the surface of a small ice accretion near the stagnation region. On the other hand, critical roughness heights were calculated based on a single roughness element which is totally different from the roughness characteristic of the current study. Therefore, a caution is needed when a comparison between a calculated roughness height and a measured roughness height is made. Calculated critical roughness heights are meant to be used to get a rough idea about a roughness height for a boundary layer transition.

As can be seen, roughness heights in all cases are much higher than the boundary layer thickness and critical roughness heights, implying that roughness elements at measurement locations might cause a transition. However, the assumption used to calculate the critical roughness height is based on a single element which is quite different from the condition of the current study. Whether this height indeed causes a transition needs to be investigated further through detailed boundary layer measurements with the same roughness size and spacing. As discussed earlier for the airspeed effect, note that the boundary layer thickness and the critical roughness height become smaller with increasing airspeed, which makes a constant roughness height bigger relative to the boundary layer thickness (Figs. 4(a) to (c)).

In Fig. 4, measured roughness heights are plotted at the beginning of the rough zone for each icing condition. Therefore, information on the width of the smooth zone can be obtained from these surface locations where measured roughness heights are plotted. It can be seen that at colder temperatures, increasing airspeed and increasing LWC move the beginning of the rough zone closer to the stagnation region. These findings are consistent with earlier findings by Hansman, et al. (Ref. 14) on a cylinder.

Effects of Accretion Time

In this section, measurement results of the roughness height, diameter and spacing are presented at several accretion times to study roughness development with time. Measured values are listed in Table 3. As a base case, a glaze ice condition with a moderate LWC (0.5 g/m^3) and MVD (20 mm) was tested for 1, 2, 3, and 6 min. Two other conditions for a higher airspeed and a higher air temperature were tested to make a comparison with the base icing condition. For these two conditions, only 2 and 6 min ice accretions were available for the measurement.

Figure 5 shows roughness heights of the three icing conditions at various accretion times. Measurements were all made at the surface roughness transition region. As can be seen with the base case, the height grows quite rapidly during the first 2 min then very slowly between 2 and 3 min, and the height decreases slightly after 3 min. The other two icing conditions also show either no change or a slight increase in the height between 2 and 6 min. Without the data during the first 2 min and at 3 min for the higher airspeed and higher temperature icing conditions, it is difficult to draw any definite conclusion about the roughness height growth characteristic with time. However it appears that there are definitely two different growth rates: a rapid growth rate during the early stage and a very slow or even possibly a zero rate during the later stage of the ice accretion process. This result provides a contradictory view about a popular notion of continuous growth of roughness size with time.

Figure 6 shows the roughness heights of the base case at all four accretion times plotted with the boundary layer thickness and the predicted critical roughness height for a transition. It shows that roughness at 1 min protrudes above the boundary layer but it has not quite grown out of the predicted critical roughness height whereas the roughness heights at 2 and 3 min are well above the boundary layer thickness and the critical roughness height. Another important observation is that the rough zone hardly moved toward the stagnation region between 1 and 3 min although the roughness height continued to grow during a whole time. Based on these two observations, it is plausible to assume that an onset of the physical mechanism which moves the rough zone toward the stagnation region occurs after the roughness reaches a critical height which is significantly higher than the boundary layer thickness (in this case about four times higher than the boundary layer thickness), and once this mechanism takes place, roughness grows much slower or stops growing as discussed earlier. This finding provides useful guidance for future studies to understand roughness development at the surface roughness transition region and its interaction with the boundary layer. One could also utilize this information to estimate a roughness

height at any time during a very early stage of an ice accretion by interpolating the heights at the zero time and at the time when the height growth slows down or stops.

Since data on characteristics of roughness size growth and rough zone movement is not available within the first minute of the ice accretion process, there is a possibility that the physical mechanism which moves the rough zone toward the stagnation region exists even with very small roughness within the first minute. So, the rough zone started further downstream initially and moved up to the surface location documented here at 1 min. If this occurred during the first minute, the current results indicate that, for some reason, the rough zone hardly moved during the next two minutes while roughness continued to grow. Although it seems unlikely to be the case, further investigation is desirable to study roughness development during a very early stage of ice accretion processes.

Reasons for Selecting the Surface Roughness Transition Region for Measurements

There were several reasons for selecting this surface location for the measurements. First, it is a very important region in terms of roughness and boundary layer development. One of the questions which has precipitated many discussions is what causes a distinct difference in the surface condition at this region. One of the theories (Ref. 4) is that a water film forms stationary beads due to surface tension causing a transition in the boundary layer, which enhances heat transfer and freezes the water beads. Although it is plausible, there has not been any investigation to find whether a boundary layer transition indeed takes place at the beginning of the rough zone. In order to address this question, it is necessary to make detailed boundary layer measurements over a rough surface with the same kind of surface condition as an actual ice accretion. For this, it is essential to understand the roughness characteristics in this region. Secondly, it was found during the data analysis that the roughness size does not change along the surface in the rough zone. Therefore it was not a concern where measurements need to be made.

Having stated that roughness size remains unchanged in the rough zone, more discussion is necessary to understand the definitions of roughness and the rough zone used in the current study. Olsen and Walker (Ref. 9) said that roughness grows with time, which is found to be true from the results of this study at least until a critical roughness size is reached. However, digital images show that there are two types of growth. One is macro-growth responsible for forming a main ice shape with horns and feathers. The other is micro-growth responsible for forming roughness on the surface of the macro ice shape. An illustration of roughness and ice shape development is given in Fig. 7. At the initial stage of an ice accretion (Fig. 7(a)), roughness develops on an ice substrate which has a fairly uniform thickness (See regions A and B). Small ice bumps at various spots grow aft of the rough zone (region C) in what is commonly referred to as a feather region. In the feather region, there is no ice substrate.

As the ice accretion process continues (Fig. 7(b)), the rough zone propagates toward the stagnation region, and the roughness size at the surface roughness transition region (region A) grows to a critical size as discussed earlier. Roughness elements in region B continue to grow, eventually forming a major ice structure commonly referred to as a horn. The horn grows to have its own hills and valleys along the span, however these hills and valleys are much bigger in size compared to the roughness in the surface roughness transition region. As this major horn structure develops, roughness elements whose size is almost the same as roughness elements in the surface roughness transition region develop on the horn surface. This phenomenon has not been revealed until digital images with high magnification of the current study showed detailed surface conditions and the measurement technique provided an ability to quantify the roughness size. Feathers in the region C also continue to grow with time. Some feathers near the horn merge into the main ice structure adding mass and altering the ice shape, and feathers further downstream grow individually although they may merge with each other forming a bigger feather. Regardless of where these feathers grow and how they merge together, an ice substrate does not develop in the feather region. Also, the size of these feathers is an order of magnitude bigger than the roughness size in the region A and B.

These findings and observations clearly suggest that macro irregularity of the surface in the horn area and feather growth should not be considered as roughness rather they need to be considered as part of an overall ice shape which need to be calculated in the ice accretion model. The definition used for roughness during this study is that roughness is surface irregularity growing on top of the macro ice shape. Also, the definition of the rough zone for the current study is the region where the roughness exists as illustrated in the regions A and B in Fig. 7. It is also apparent that investigations are needed to understand how small initial roughness elements in region B grow to form a large horn structure, and to understand how small roughness elements develop on the horn surface.

Roughness Characteristics Along the Surface

As mentioned in the Introduction, the study of ice roughness has another importance in providing information about surface characteristics for aerodynamic tests with simulated ice shapes. For this, detailed documentation of all surfaces over the ice accretion must be obtained. This kind of documentation also provides understanding of how the surface condition changes during an ice accretion process. A glaze ice accretion and a rime ice accretion are presented to illustrate the obvious difference between the two in accretion physics and the surface condition. The results are presented for 2 and 6 min accretions for a comparison of the surface condition with time. Test conditions are listed in Table 1.

Figure 8(a) shows the glaze ice shapes for 2 and 6 min ice accretions. While at 2 min, horn development is not quite evident, at 6 min, horns are clearly grown on both sides of the airfoil. Feathers grew normal to the surface at 2 min, but they grew into the local flow direction in the region near the icing limit at 6 min. Even at 6 min, feathers right behind the horn were growing more normal to the surface, which made these feathers merge into the horn.

Rime ice shapes are shown in Fig. 8(b). Unlike glaze ice, incoming water drops freeze on impact with no runback due to sufficient heat transfer, resulting in a shape more like an extension of the leading edge with an absence of horn development. Feathers distinctly grew into the local flow direction. It should be noted that structure of rime ice feathers is different from that of glaze ice feathers.

Measurements were made at the surface roughness transition region, horn area, and the feather region and measured mean values are listed in Table 4. Since digital images for height measurements at the horn area were not available, height information at the horn area is inferred from diameter measurements. Mean values of the feather height for the glaze ice accretions are all measured where feathers grow normal to the surface. However because of rime feather growth pattern, mean values presented in Table 4 for rime feathers simply represent the length of the feather growing into the local flow direction.

Also it should be noted that the feather height or length was measured from the airfoil surface whereas roughness height at the surface roughness transition and horn regions were measured from the top of the ice substrate. It is apparent that feathers are much bigger in size than roughness, which confirms the earlier discussion of the definition of roughness versus ice shape.

It is known that friction drag dominates the airfoil drag with a small ice accretion where surface roughness affects the boundary layer. However, with a bigger ice accretion with horns, pressure drag dominates the airfoil drag by changing the pressure distribution around the leading edge. Ice accretion codes available to date do not account for feather growth and its contribution to the horn growth. Therefore if an ice shape predicted by these ice accretion codes is used for calculating aerodynamic degradation, effects due to the presence of the feather structure is ignored. With the current observation of the surface condition, it is plausible that the aerodynamic degradation due to the feather structure can be significant, and this might explain why previous studies (Refs. 14 and 16) predicted lower airfoil drag compared with the measured drag for large glaze ice shapes.

Summary

Characteristics of surface roughness associated with leading edge ice accretions have been presented. The results were analyzed for the effects of icing parameters and the effect of accretion time. Major findings are:

(1) The roughness height increases with warmer temperatures and increasing LWC. These results show the same trend as the current LEWICE sand grain roughness model (Ref. 12) predicts.

(2) The airspeed has little effect on the roughness height; however, relative roughness height to the boundary layer thickness increases with increasing airspeed as the thickness of the boundary layer decreases.

(3) Colder temperatures, increasing airspeed, and increasing LWC move the beginning of the rough zone closer to the stagnation region.

(4) Measured roughness heights with 2 min ice accretions are 3 to 5 times larger than calculated clean airfoil boundary layer thicknesses at the surface roughness transition region. Although calculated boundary layer thicknesses are based on somewhat different leading edge geometry and surface conditions, a magnitude of measured roughness heights suggests that roughness elements at the surface roughness transition region probably protrude well out of the boundary layer and possibly cause a boundary layer transition.

(5) It is found that the roughness growth rate can be quite different between an initial stage and a later stage of an accretion process. The current result suggests rapid initial growth followed by much slower growth or possibly zero growth.

(6) It is found that roughness develops on the surface of horn structure which has its own macro surface irregularity. The relation between the macro ice shape growth and micro roughness growth needs to be explored further. Feather structure downstream of the horn area should be considered as part of the macro ice shape, and irregular surface conditions due to the feather growth need to be accounted for by the ice accretion model, not by a roughness model.

The analyses of roughness heights, boundary layer thicknesses, and predicted critical roughness heights conducted by the current study suggest a boundary layer transition occurring at the boundary between the smooth and the rough zones. However, a definite conclusion is not possible due to the use of a clean surface condition and a simpler roughness charac-

teristic for calculating boundary layer thicknesses and critical roughness heights. In order to understand the underlying physics, thorough investigation is needed through detailed and carefully devised boundary layer measurements over realistic rough surfaces. Results from such tests are believed to be able to answer the question of what fixes the roughness and allows it to grow outward and toward the stagnation region.

References

1. Nikuradse, J., "Strömungsgesetze in Rauher Rohen," VDI-Forschungsheft 361, 1933. (Also "Laws of Flow in Rough Pipes," NACA TM–1292).
2. Schlichting, H., "Experimentelle Untersuchungen zum Rauhigkeitsproblem,"*Ingenieur-Archiv VII*, Vol. 1, 1936, pp. 1–34. (Also "Experimental Investigation of the Problem of Surface Roughness," NACA TM–823).
3. Olsen, W. and Walker, E., "Experimental Evidence for Modifying the Current Physical Model for Ice Accretion on Aircraft Surfaces," NASA TM–87184, 1986.
4. Hansman, R.J., Yamaguchi, K., Berkowitz, B., and Potapczuk, M., "Modeling of Surface Roughness Effects on Glaze Ice Accretion," AIAA Paper 89–0734, January, 1989.
5. Hansman, R.J., "Analysis of Surface Roughness Generation in Aircraft Ice Accretion," AIAA Paper 92–0298, January, 1992.
6. Hansman, R.J., Breuer, K.S., Hazan, D., Reehorst, A., and Vargas, M, "Close-up Analysis of Aircraft Ice Accretion," AIAA Paper 93–0029, January, 1993.
7. Brumby, R.E., "The Effect of Wing Ice Contamination on Essential Flight Characteristics," AGARD Conference Proceedings on Effects of Adverse Weather on Aerodynamics, pp. 2–1 to 2–4, AGARD–CP–496, December, 1991.
8. Lynch, F.T., Valarezo, W.O., and McGhee, R.J., "The Adverse Aerodynamic Impact of Very Small Leading-Edge Ice (Roughness) Buildups on Wings and Tails," AGARD Conference Proceedings on Effects of Adverse Weather on Aerodynamics, pp. 12–1 to 12–8, AGARD–CP–496, December, 1991.
9. Oolbekkink, B. and Volkers, D.F., "Aerodynamic Effects of Distributed Roughness on a NACA 632-015 Airfoil," AIAA Paper 91–0443, January, 1991.
10. Adobe Photoshop, Adobe Systems Incorporated, 1990.
11. IPLab Spectrum, Signal Analytics Corporation, 1992.
12. Ruff, G.A., and Berkowitz, B.M., "Users Manual for the NASA Lewis Ice Accretion Code (LEWICE)," NASA CR–185129, 1990.
13. Gent, R.W., Markiewicz, R.H., and Cansdale, J.T., "Further Studies of Helicopter Rotor Ice Accretion and Prediction," Paper No. 54, Eleventh European Rotorcraft Forum, September, 1985.
14. Shin, J., Berkowitz, B., Chen, H., and Cebeci, T., "Prediction of Ice Shapes and Their Effect on Airfoil Performance," AIAA Paper 91–0264, January, 1991.
15. Bragg, M.B., Kerho, M., and Winkler, J., "Effect of Initial Ice Roughness on Airfoil Aerodynamics," AIAA Paper 94–0800, January, 1994.
16. Potapczuk, M. and Al-Khalil, K.M., "Ice Accretion and Performance Degradation Calculations with LEWICE/NS," AIAA Paper 93–0173, January, 1993.

Table 1. Test Conditions

(a) Effects of Icing Parameters

Category	Airspeed, m/s	Total Temperature, °C	LWC, g/m^3	MVD, μm	Accretion Time, minute
Airspeed Effect	67.1	-2.2	0.5	20	2
	89.5	"	"	"	"
	111.8	"	"	"	"
Temperature Effect	67.1	-1.1	0.5	"	"
	"	-2.2	"	"	"
	"	-3.9	"	"	"
LWC Effect	67.1	-2.2	0.5	"	"
	"	"	0.75	"	"
	"	"	1.0	"	"
	"	"	1.2	"	"

(b) Effects of Accretion Time

Category	Airspeed, m/s	Total Temperature, °C	LWC, g/m^3	MVD, μm	Accretion Time, minute
Base Case	67.1	-2.2	0.5	20	1
	"	"	"	"	2
	"	"	"	"	3
	"	"	"	"	6
Higher Airspeed	111.8	-2.2	0.5	20	2
	"	"	"	"	6
Higher Temperature	67.1	-1.1	0.5	20	2
	"	"	"	"	6

Table 1. Test Conditions (continued).

(c) Roughness Characteristics Along the Surface

Category	Airspeed, m/s	Total Temperature, °C	LWC, g/m^3	MVD, μm	Accretion Time, minute
Glaze Ice	67.1	-1.1	0.5	20	2
	"	"	"	"	6
Rime Ice	111.8	-17.2	0.5	20	2
	"	"	"	"	6

Table 2. Measured Roughness Size for Effects of Icing Parameters.

Note: A symbol √ indicates a data point with a bad height image. Height information is inferred from the diameter measurement.

Airspeed, m/s	Height, mm	Diameter, mm	Spacing, mm	Width of Smooth Zone, mm
67.1 (150 mph)	0.57 (0.01)	1.11 (0.20)	1.28 (0.14)	6.0
89.5 (200 mph)	0.58 (0.07)	1.05 (0.11)	1.28 (0.07)	5.0
111.8 (250 mph)	0.58 (√)	1.06 (0.12)	1.19 (0.09)	4.0

Total Temperature, °C	Height, mm	Diameter, mm	Spacing, mm	Width of Smooth Zone, mm
-1.1 (30 °F)	0.62 (0.09)	1.33 (0.27)	1.45 (0.17)	8.0
-2.2 (28 °F)	0.57 (0.01)	1.11 (0.20)	1.28 (0.14)	6.0
-3.9 (25 °F)	0.51 (0.06)	0.93 (0.11)	1.02 (0.25)	6.0

LWC, g/m^3	Height, mm	Diameter, mm	Spacing, mm	Width of Smooth Zone, mm
0.5	0.57 (0.01)	1.11 (0.20)	1.28 (0.14)	6.0
0.75	0.61 (√)	1.22 (0.18)	1.48 (0.11)	5.5
1.0	0.74 (0.04)	1.42 (0.16)	1.59 (0.23)	5.0
1.2	0.79 (0.07)	1.56 (0.19)	1.71 (0.04)	4.5

Table 3. Measured Roughness Size for Effects of Accretion Time.

Note: A symbol √ indicates a data point with a bad height image. Height information is inferred from the diameter measurement.

(a) Base Condition

Accretion Time, minute	Height, mm	Diameter, mm	Spacing, mm	Width of Smooth Zone, mm
1	0.28 (0.06)	0.56 (0.07)	0.56 (0.07)	7.0
2	0.57 (0.01)	1.11 (0.20)	1.28 (0.14)	6.0
3	0.62 (0.03)	1.15 (0.11)	1.33 (0.14)	6.0
6	0.55 (0.08)	1.05 (0.11)	1.18 (0.11)	3.5

(b) Higher Airspeed

Accretion Time, minute	Height, mm	Diameter, mm	Spacing, mm	Width of Smooth Zone, mm
2	0.58 (√)	1.06 (0.12)	1.19 (0.09)	4.0
6	0.57 (0.05)	1.15 (0.07)	1.32 (0.11)	0.0

(c) Higher Total Temperature

Accretion Time, minute	Height, mm	Diameter, mm	Spacing, mm	Width of Smooth Zone, mm
2	0.62 (0.09)	1.33 (0.27)	1.45 (0.17)	8.0
6	0.63 (0.04)	1.21 (0.11)	1.39 (0.14)	5.0

Table 4. Measured Roughness Size for Roughness Characteristics along the Surface

Notes: 1) A symbol ‡ indicates that height information is inferred from diameter measurements due to unavailable height images.
2) NA notes for not available.

(a) Glaze Ice

	2 Minute Ice Accretion	6 Minute Ice Accretion
Width of Smooth Zone, mm	6	3.5
Height at Surface Roughness Transition Region, mm	0.57	0.55
Height at Horn Region, mm	0.57(‡)	0.64 (‡)
Mean Feather Height, mm	1.20	2.3
Feather Height Range, mm	1.09 ~ 1.38	1.68 ~ 3.42
Feather Growth Direction	normal to the flow	normal to the flow (right behind the horn) parallel to the flow (further downstream)
Icing Limit, mm	20 ~ 25	30 ~ 35

(b) Rime Ice

	2 Minute Ice Accretion	6 Minute Ice Accretion
Width of Smooth Zone, mm	5.0	5.0
Height at Surface Roughness Transition Region, mm	0.17	0.21
Height at Horn Region, mm	NA	NA
Mean Feather Length, mm	2.45	7.04
Feather Length Range, mm	2.05 ~ 2.85	6.28 ~ 7.80
Feather Growth Direction	parallel to the flow	parallel to the flow
Icing Limit, mm	NA	NA

Figure 1. Plan View of Roughness.

Figure 2. Profile View of Roughness.

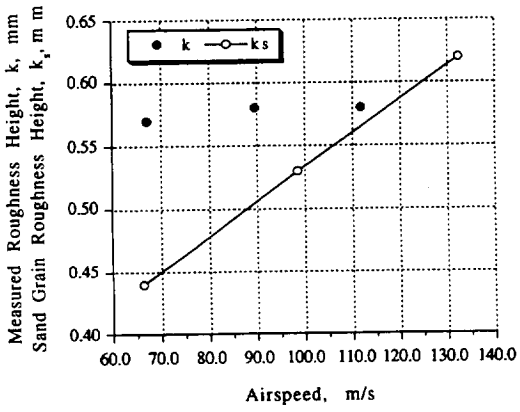

(a)

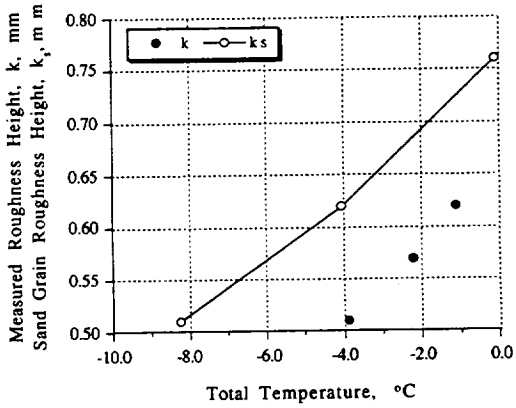

(b)

Figure 3. Comparison of Measured Roughness Height, k, with Sand Grain Roughness Height, k_S, Predicted by LEWICE roughness Model (continued).

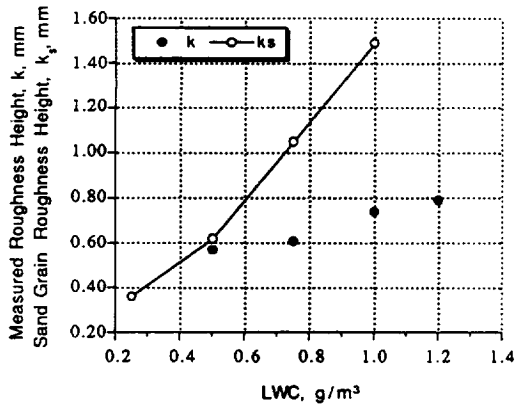

(c)

Figure 3. Comparison of Measured Roughness Height, k, with Sand Grain Roughness Height, k_s, Predicted by LEWICE roughness Model.

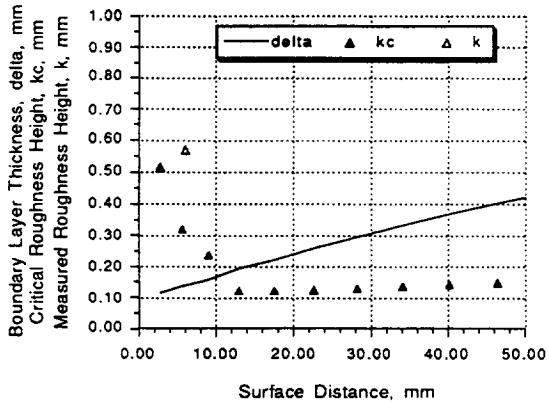

(a) V_∞ = 67.1 m/s

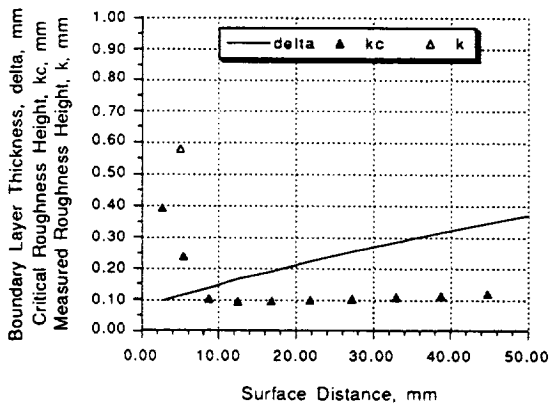

(b) V_∞ = 89.5 m/s

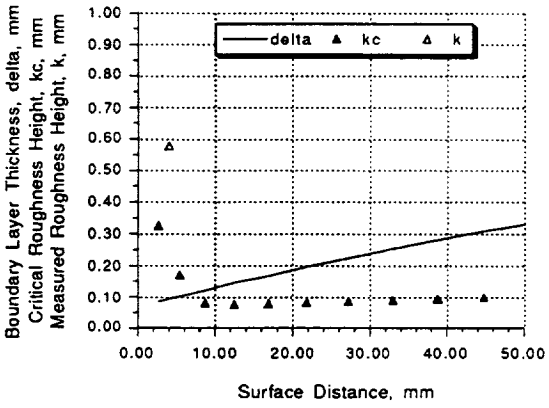

(c) V_∞ = 111.8 m/s

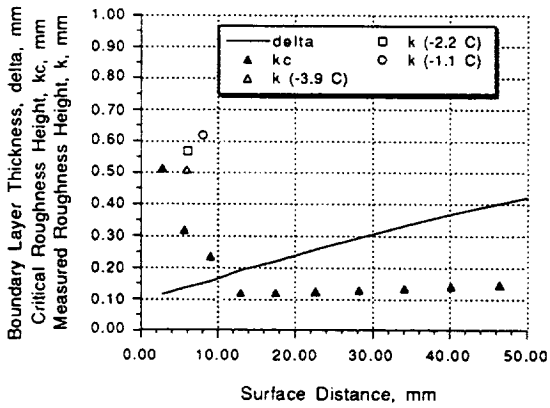

(d) Temperature Effect

Figure 4. Comparison of Measured Roughness Height with Boundary Layer Thickness and Critical Roughness Height (continued).

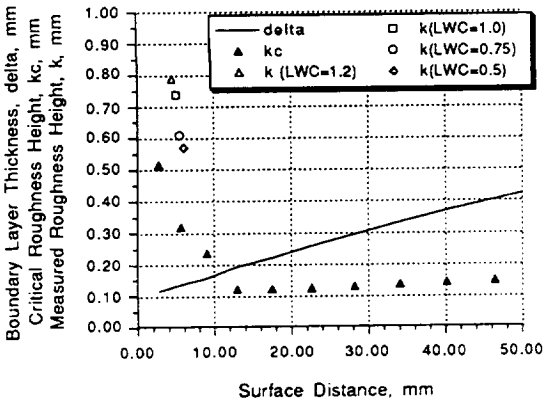

(e) LWC Effect

Figure 4. Comparison of Measured Roughness Height with Boundary Layer Thickness and Critical Roughness Height.

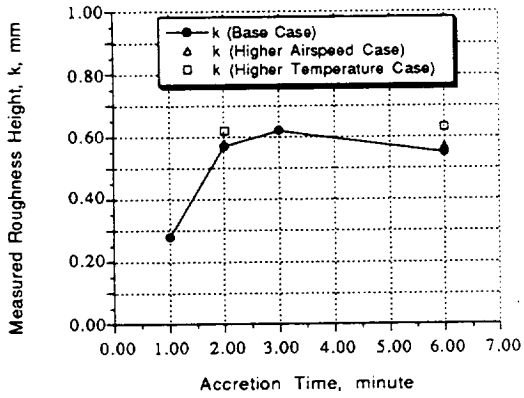

Figure 5. Effects of Accretion Time on Roughness Height.

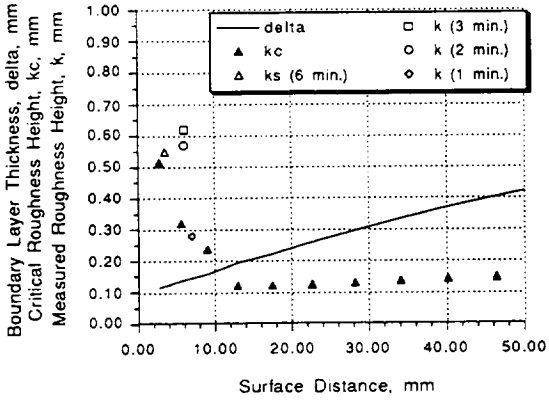

Figure 6. Comparison of Measured Roughness Height with Boundary Layer.

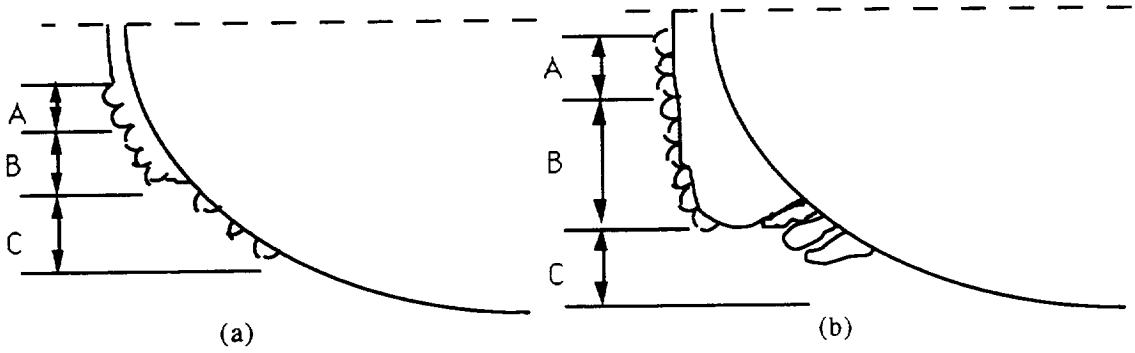

Figure 7. Illustration of Ice Shape and Roughness Growth.

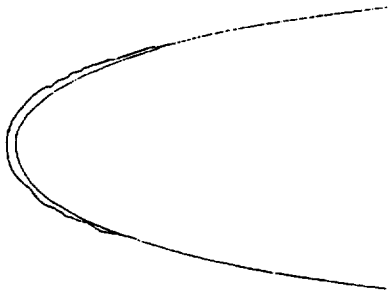

(a) Glaze Ice, t = 2 minute

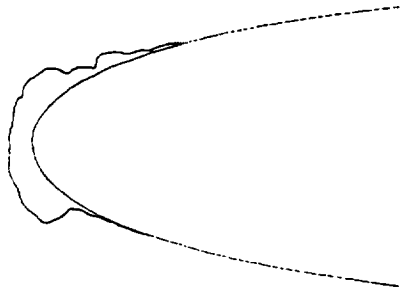

(b) Glaze Ice, t = 6 minute

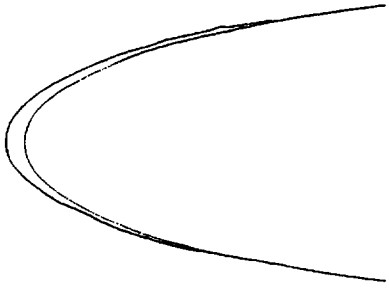

(c) Rime Ice, t = 2 minute

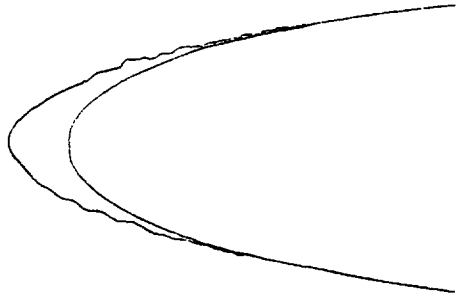

(d) Rime Ice, t = 6 minute

Figure 8. Traced Ice Shapes.

REPORT DOCUMENTATION PAGE

Form Approved
OMB No. 0704-0188

1. AGENCY USE ONLY (*Leave blank*)	2. REPORT DATE	3. REPORT TYPE AND DATES COVERED
	January 1994	Technical Memorandum

4. TITLE AND SUBTITLE

Characteristics of Surface Roughness Associated With Leading Edge Ice Accretion

5. FUNDING NUMBERS

WU-505-68-10

6. AUTHOR(S)

Jaiwon Shin

7. PERFORMING ORGANIZATION NAME(S) AND ADDRESS(ES)

National Aeronautics and Space Administration
Lewis Research Center
Cleveland, Ohio 44135-3191

8. PERFORMING ORGANIZATION REPORT NUMBER

E-8320

9. SPONSORING/MONITORING AGENCY NAME(S) AND ADDRESS(ES)

National Aeronautics and Space Administration
Washington, D.C. 20546-0001

10. SPONSORING/MONITORING AGENCY REPORT NUMBER

NASA TM-106459
AIAA-94-0799

11. SUPPLEMENTARY NOTES

Prepared for the AIAA 32nd Aerospace Sciences Meeting sponsored by the American Institute of Aeronautics and Astronautics, Reno, Nevada, January 10-13, 1994. Responsible person, Jaiwon Shin, (216) 433-8714.

12a. DISTRIBUTION/AVAILABILITY STATEMENT

Unclassified - Unlimited
Subject Category 02

12b. DISTRIBUTION CODE

13. ABSTRACT ***(Maximum 200 words)***

Detailed size measurements of surface roughness associated with leading edge ice accretions are presented to provide information on characteristics of roughness and trends of roughness development with various icing parameters. Data was obtained from icing tests conducted in the Icing Research Tunnel (IRT) at NASA Lewis Research Center (LeRC) using a NACA 0012 airfoil. Measurements include diameters, heights, and spacing of roughness elements along with chordwise icing limits. Results confirm the existence of smooth and rough ice zones and that the boundary between the two zones (surface roughness transition region) moves upstream towards stagnation region with time. The height of roughness grows as the air temperature and the liquid water content increase, however the airspeed has little effect on the roughness height. Results also show that the roughness in the surface roughness transition region grows during a very early stage of accretion but reaches a critical height and then remains fairly constant. Results also indicate that a uniformly distributed roughness model is only valid at a very initial stage of the ice accretion process.

14. SUBJECT TERMS

Surface roughness; Ice accretion; Image processing

15. NUMBER OF PAGES

18

16. PRICE CODE

A03

17. SECURITY CLASSIFICATION OF REPORT	18. SECURITY CLASSIFICATION OF THIS PAGE	19. SECURITY CLASSIFICATION OF ABSTRACT	20. LIMITATION OF ABSTRACT
Unclassified	Unclassified	Unclassified	